

Effect of Impregnation of Activated Carbon with Selected Transition Metal Ions on Its Adsorption Properties and Pore Size

POSZWALD Bartosz^{1,a*}, KWAK Anna^{1,b}, DYSZ Karolina^{1,c}
and DYLONG Agnieszka^{1,d}

¹ Military Institute of Engineer Technology, 136 Obornicka Str., 50-961 Wrocław, Poland

^a poszwald@witi.wroc.pl, ^b kwak@witi.wroc.pl, ^c dysz@witi.wroc.pl, ^d dylong@witi.wroc.pl

Keywords: Activated Carbon, Impregnation, Adsorption Isotherm, BET Method, BJH Method, Transition Metals

Abstract. Thanks to their vast surface area, activated carbons are materials of great interest. They are used as adsorbents for both liquid- and gaseous impurities. To improve their properties, impregnation with different substances is conducted. In this paper, such an impregnation was done using copper(II), manganese(II), silver(I), and zinc(II) salts. The aim was to compare the inner structure of the impregnated activated carbon with a non-impregnated one. It was done by Brunauer-Emmett-Teller (BET) adsorption-desorption isotherms that were plotted and described. Lastly, the pore size and volume were determined by Barrett-Joyner-Halenda (BJH) method. The results show that the presence of zinc(II) salts helped to develop the mesoporous structure of activated carbon and resulted in an increase in the surface area of the sorbents, while silver(I) decreased it.

Introduction

Adsorption is a process taking place at the interphase phases [1]. It can be physical and involve covalent bonds, ionic bonds, van der Waals forces, or chemical in character when adsorbate is reacting with adsorbent [2]. The efficiency of the process is highly dependent on how large the surface area of the sorbent is. Many factors may impact this parameter but one of them, more than any other is meaningful – the porosity. Pores are cavities on the surface of a sorbent which multiply its surface by manyfold. Zeolite can serve as an example here, with its surface of almost 130 m²/g [3], or activated carbon with 2636 m²/g [4].

Continues process of absorption can be described using graphs called isotherms, showing the relationship between the amount of adsorbed substance and its concentration in an equilibrium state. Many isotherms describe different theories and states. For example, Henry's isotherm is adequate for the process of adsorption of low-concentration fluids and gases, and the Freundlich model is describing a situation in which the surface of the adsorbent is not smooth but porous. One of the most used, thanks to its great adequacy to reality, is Brunauer-Emmett-Teller (BET) theory. Its main assumption is based on Langmuir isotherm [5] but modified, so it is describing a multilayer adsorbate on a porous sorbent's surface. The important thing here is the fact, that the greater the vapour pressure of adsorbate over adsorbent, the higher the number of adsorbed particles. BET is given by a linear equation (Eq. 1) but following further mathematical operations BET isotherms are curves.

$$\frac{1}{X\left(\frac{p_0}{p} - 1\right)} = \frac{1}{X_m C} + \frac{C - 1}{X_m C} \left(\frac{p}{p_0}\right) \quad \text{Eq. 1}$$

X – the total adsorbed volume of gas under pressure p

p_0 – saturated vapor pressure of an adsorbate

X_m – monolayer capacity (volume of gas adsorbed in a single layer)
 C – equilibrium adsorption state

By knowing the monolayer capacity from the equation (Eq. 1) total surface of the adsorbent can be calculated (Eq. 2):

$$S = \frac{X_m L_{Av} A_m}{M_v} \quad \text{Eq. 2}$$

S – total surface area

L_{av} – Avogadro’s number

A – cross-sectional area of the adsorbate (for nitrogen 0.162 nm²)

M_v – molar volume

Six types of isotherms can be described, according to the International Union of Pure and Applied Chemistry (IUPAC) [6]. They are depicting (Fig. 1) the adsorption process on different adsorbents with variable pore structures, divided into both pore size and pore shape. Designations (names) for pores by size are determined by IUPAC, a micropore is less than 2nm cavity, a mesopore ranges from 2 to 50 nm, and a macropore is larger than 50 nm. Pore size also affects the condensation mechanism. While there is three-dimensional condensation in micropores and capillary condensation in mesopores, there is no condensation in macropores [7].

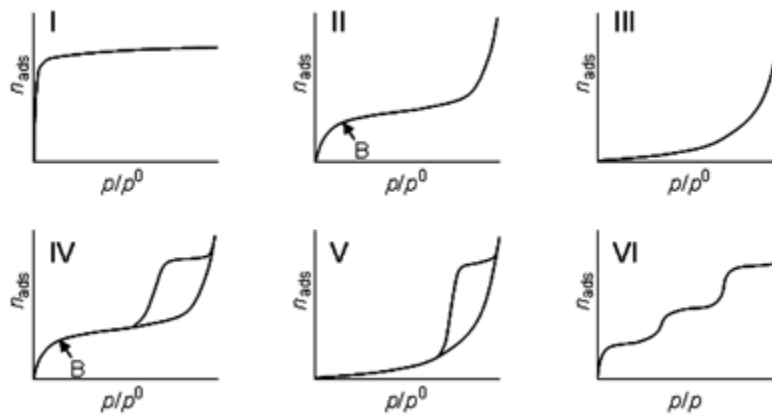


Fig.1. Types of isotherms by adsorbent outer structure. Type I: microporous; type II: non-porous or macroporous; type III: non-porous or macroporous but with weak interactions; type IV: mesoporous; type V: mesoporous but with weak interactions; type VI: step-by-step multilayer adsorption. (source: [8]).

Activated carbons (ACs) are being used in many fields. They are obtained from organic matter, through a process called activation. Among the most popular substrates are wood (35% of total substrates used), coal (28%), lignite (14%), peat (10%), and local organic residues such, as coconut shells or fruit stones (10%). Activation can be divided into two types: chemical one and physical one. The former involves two steps, the first step includes mixing the substrate with some reagents, e.g. zinc(II) chloride, phosphoric acid or sodium hydroxide, and the second one is heating. Activation temperature depends on the type of substance that was used. Carbon mixed with ZnCl₂ is heated to around 600°C, at which temperature total dehydration takes place. On the other hand, substrates containing H₃PO₄ are heated to 800°C, so that the acid is oxidizes carbon and the structure is changing [9]. Physical activation is heating conducted in two steps. In the beginning, the substrate is carbonized at 400-600°C, as in this temperature rigid carbon structure is obtained.

To get the actual, useful product oxidation has to take place. It is done by increasing the temperature to 800-950°C with the addition of water vapour or carbon dioxide to the reaction environment, which penetrates and expands pores [10]. Such products can be further modified by impregnating them with different compounds so the ACs' properties are altered or upgraded. Metal-impregnated activated carbons (MIACs) are sorbents of great interest due to their relatively simple manufacturing.

Experimental Procedure

DT0 commercially-available activated carbon (produced by Gryfskand Sp. z o.o. company in Poland) was used in this experiment. It was first oxidized in a 20% nitric acid solution and then washed until all the acid was removed. Afterwards, a washed activated carbon was kept at room temperature for 24h. At the end of the process, the product was dried in a fluid bed dryer at 120°C.

The following transition metal salts were chosen for impregnation

- universal adsorbents (UA), containing zinc, copper, manganese, silver, and
- adsorbents containing zinc and silver (S-Hg/Pb) only.

The following metallic catalysts have been selected to produce UA:

- basic copper carbonate ($Cu_2CO_3(OH)_2$) in aqua ammonia;
- potassium permanganate ($KMnO_4$) in aqueous solution;
- silver nitrate ($AgNO_3$) in aqueous solution;
- zinc nitrate ($ZnNO_3$) in aqueous solution.

The final step leading to MIACs possessing the desired properties was drying them for 6 hours at the temperature of 120°C and 2 hours at 180°C.

Adsorption-desorption isotherms and inner structure tests were carried out on Autosorb-1C chemisorption - physisorption analyzer by Quantachrome Instruments.

Table 1. Concentrations of metal ions in MIACs

No.	Sorbent	Copper(II) [% w/w]	Manganese(II) [% w/w]	Silver(I) [% w/w]	Zinc(II) [% w/w]
1.	DT0	-	-	-	-
2.	IS-2	3.0	1.2	0.5	1.0
3.	IS-3	3.0	1.2	-	0.5
4.	IS-4	3.0	1.2	0.5	2.0
5.	IS-5	3.5	1.8	1.0	-
6.	IS-6	3.0	1.8	1.0	-
7.	IS-7	3.0	1.8	0.5	-
8.	IS-8	3.0	1.2	0.5	-
9.	IS-9	3.0	1.2	1.0	-
10.	IS-10	2.5	1.2	0.5	-

Results and Discussion

Some of the MIACs impregnated with zinc(II) and other salts contained aggregated copper-blue particles. Those carbons were observed under Keyence series VHX-7000 microscope with VH-ZST dual objective zoom lens (Fig. 2). It seems that some regions adsorbed more copper(II) salt which, during the heating process, was not reduced to copper(II) oxide. This irregularity must be linked to the presence of zinc(II) salt in the samples, but chemistry of this process is not known yet, due to insufficient amount of data.

By comparing the surface areas of DT0 and ISs we see that zinc(II) impregnated ACs have a significantly larger surface than their nonimpregnated precursor. Other adsorbents, IS-5 – IS-10, had their area decreased by 5-10%. Additionally, the highest increase, around 44%, was noted for

IS-3 – the only sorbent which does not contain silver(I). Thus, a conclusion can be made that presence of zinc(II) salt in the impregnation mixture is promoting better performance parameters, while silver(I) presence is accomplishing the opposite.

To specify, which pores were affected the most, the BJH curve was used. It appears that zinc(II) helped to develop the mesoporous structure of activated carbon. The biggest increase is observed for IS-3 and IS-4 sorbents. This implies that the absence of silver(I) and a higher concentration of zinc(II) positively impact the efficiency of adsorption properties. As can be seen in graphs (Fig. 4 b) and c)) micropore capacity has also increased. One unusual situation was noted for IS-8 in which the mesopores disappearance almost totally.

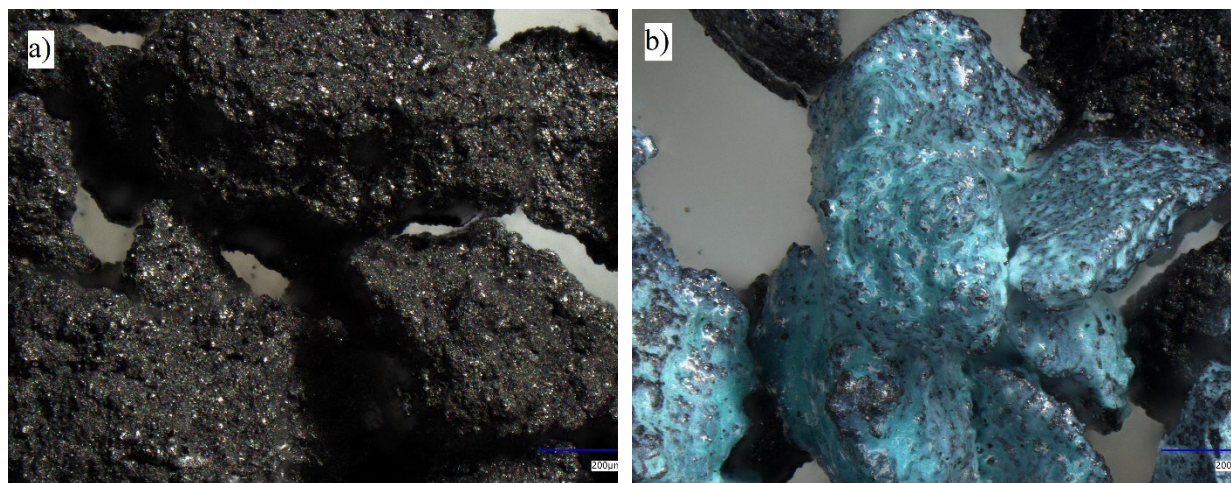


Fig.2. a) Noncoated IS-5 vs. b) copper(II) salt coated aggregated AC IS-4

While considering the changes to the structure of all the adsorbents, they are not as large as one could assume. This is proven by BET isotherms (Fig. 4), as all of them are type IV(a) with H4 hysteresis [11], which means that the shape of the pores remains unchanged and only the number of individual pores differentiates the MIACs.

Table 2. Sorbents parameters

Sample	DT0	IS-2	IS-3	IS-4	IS-5	IS-6	IS-7	IS-8	IS-9	IS-10
Surface area* [m ² /g]	555.4	796.6	804.3	592.1	523.0	507.8	491.7	498.2	482.7	519.2
Average pore size [nm]	2.100	2.139	2.346	2.296	2.117	2.106	2.076	2.114	2.115	2.112

* BJH method cumulative desorption surface area

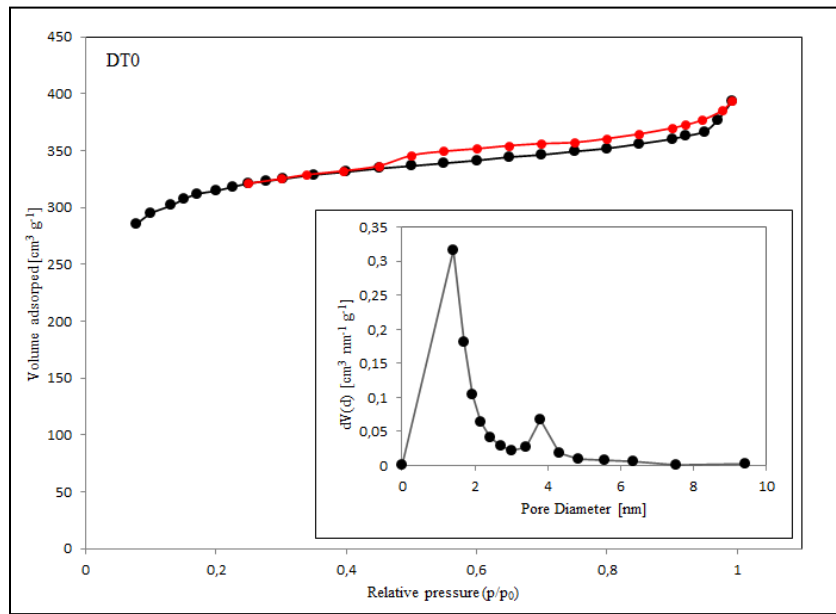
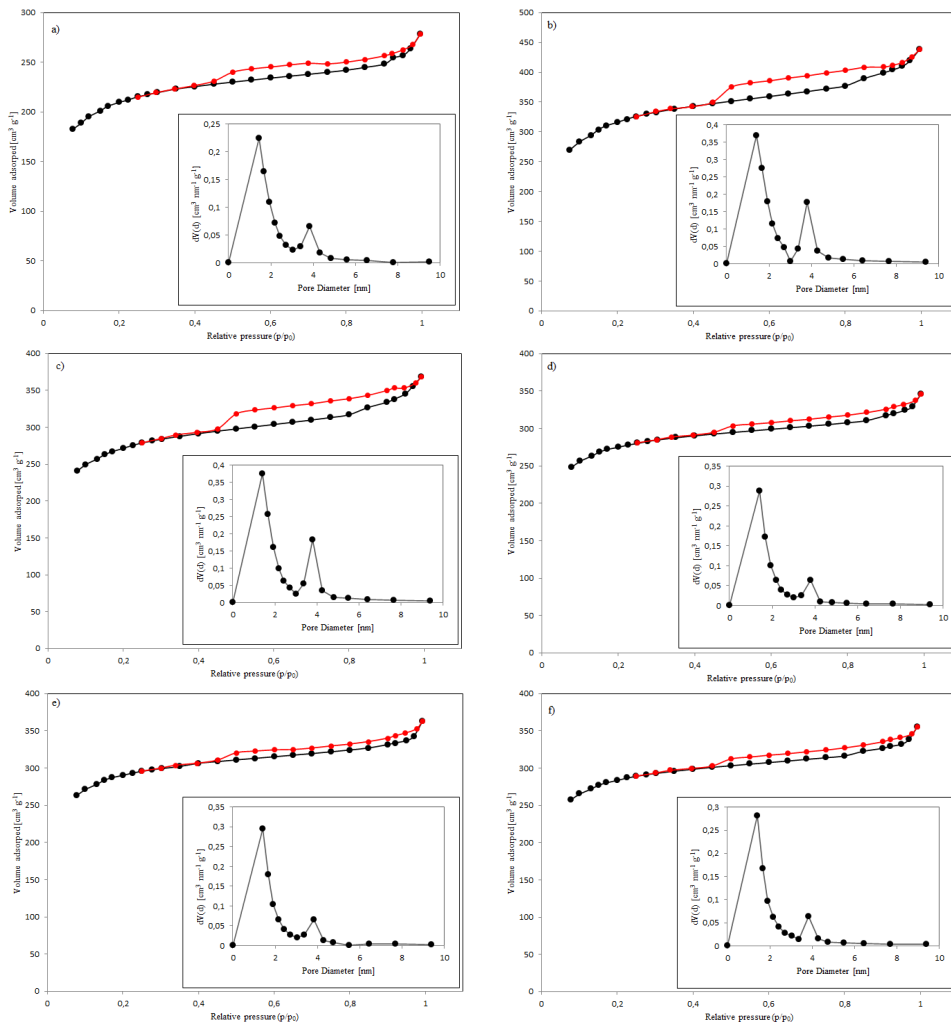


Fig.3. BET nitrogen adsorption-desorption isotherms and BJH pore size distribution curve of DT0



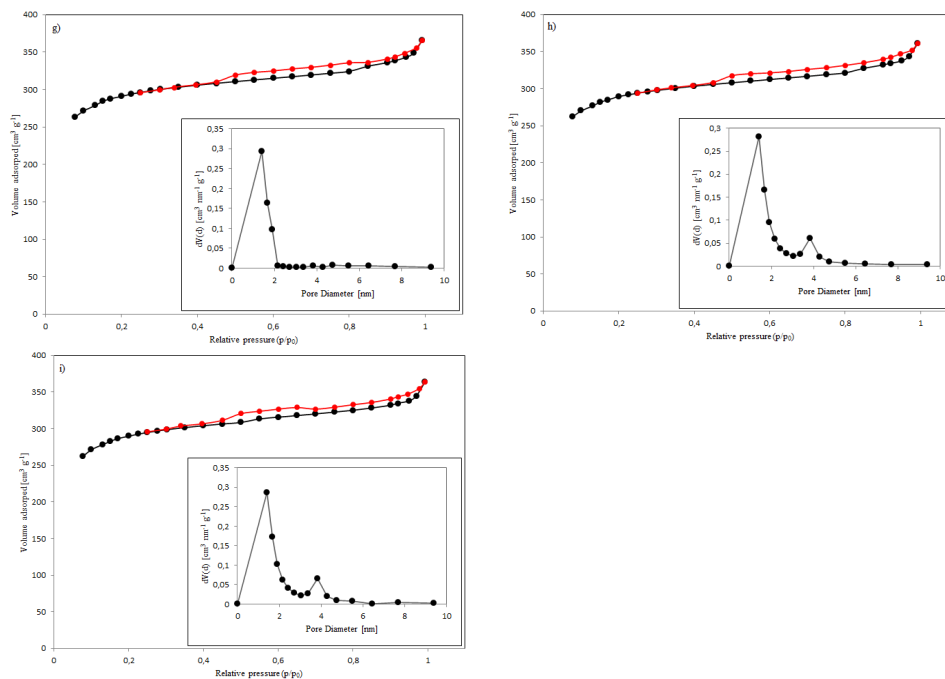


Fig.4. BET nitrogen adsorption-desorption isotherms and BJH pore size distribution curve of: a) IS-2, b) IS-3, c) IS-4, d) IS-5, e) IS-6, f) IS-7, g) IS-8, h) IS-9, i) IS-10

Conclusions

This paper proves that the introduction of transition metals salts is changing the inner structure of activated carbons. For example, silver(I) causes a decrease in the number of pores yielding so smaller surface area and resulting in worse adsorption properties. However, silver is an antiseptic so it would be helpful in the treatment of biologically-contaminated samples. On the opposite side, there is zinc(II), which increases the porosity of carbonaceous adsorbents by as high as 44%. Such modified carbons have more developed mesopores and micropores. More transition metal ions may have a positive impact on the adsorbent structure, however further experiments are required.

Any further work will require in-depth statistical analysis [12], especially regarding possible interactions [13-15]. In cases where the number of available measurements is too small to adequately narrow down the uncertainty range, nonparametric [16-18] and resampling [19, 20] approaches will be useful. The obtained results and the methodology of these approaches can be applicable in metal processing [21], welding [22], and coating applications [23], including special coatings [24, 25].

References

- [1] S.J. Chak. Absorption, in: A.D. McNaught, A. Wilkinson (Eds.) IUPAC. Compendium of Chemical Terminology 2nd ed., Blackwell Scientific Publications, Oxford, 1997.
<https://doi.org/10.1351/goldbook.A00036>
- [2] Procesy sorpcyjne. Skrypt do ćwiczeń. [online]. 2010. [viewed: 2023-01-25]. Available from: http://www2.chemia.uj.edu.pl/dydaktyka/Procesy_Sorpcyjne.pdf
- [3] G. Jozefaciuk, A. Szatanik-Kloc, A. Ambrozewicz-Nita. The Surface area of zeolite-amended soils exceed the sum of the inherent surface areas of soil and zeolites, Eur. J. of Soil Sc. 69(5) (2018) art. 12691. <https://doi.org/10.1111/ejss.12691>

- [4] A. Kumar, H. M. Jena. Adsorption of Cr(VI) from aqueous solution by prepared high surface area activated carbon from Fox nutshell by chemical activation with H₃PO₄, *J. of Env. Chem. Eng.* 5(2) (2017) 2032-2041. <https://doi.org/10.1016/j.jece.2017.03.035>
- [5] S. Tripathi, N. Arora, P. Gupta, P.A. Pruthi, K.M. Poluri, V. Pruthi. Microalgae: An emerging source for mitigation of heavy metals and their potential implications for biodiesel production, in: A.K. Azad, M. Rasul, *Advanced Biofuels Applications, Technologies and Sustainable Development*, Woodhead Publishing, Sawstone, 2019, pp. 97-128. <https://doi.org/10.1016/B978-0-08-102791-2.00004-0>
- [6] Standardized reporting of gas adsorption isotherms [online]. 2021. [viewed: 2023-01-27]. Available from: <https://iupac.org/project/2021-016-1-024>
- [7] R.J. White, V. Budarin, J.H. Clark, R.Luque. Tuneable porous carbonaceous materials from renewable resources, *Chem. Soc. Rev.* 38(12) (2009) 3401-3418. <https://doi.org/10.1039/b822668g>
- [8] M. Kajama. Hydrogen permeation using nanostructured silica membranes, *Sustainable Development and Planning 2015* (2015), Istanbul, Turkey, 447-456. <https://doi.org/10.2495/SDP150381>
- [9] Carbonology Chemically activated carbon. [online]. 2019. [viewd: 2023-01-29]. Available from: <https://www.desotec.com/en/carbonology/carbonology-academy/chemically-activated-carbon>
- [10] T. Borowiecki, J. Kijeński, J. Machnikowski, M. Ściążko. *Czysta energia, produkty chemiczne i paliwa z węgla- ocena potencjału rozwojowego*, Wydawnictwo Instytutu Chemicznej Przeróbki Węgla, Zabrze, 2008.
- [11] M. Thommes et al. Physisorption of gases, with special reference to the evaluation of surface area and pore size distribution (IUPAC Technical Report), *Pure Appl. Chem.* 87(9-10) (2015) 1051-1069. <https://doi.org/10.1515/pac-2014-1117>
- [12] B. Jasiewicz et al. Inter-observer and intra-observer reliability in the radiographic measurements of paediatric forefoot alignment, *Foot Ankle Surg.* 27 (2021) 371-376. <https://doi.org/10.1016/j.fas.2020.04.015>
- [13] J. Pietraszek et al. The parametric RSM model with higher order terms for the meat tumbler machine process, *Solid State Phenom.* 235 (2015) 37-44. <https://doi.org/10.4028/www.scientific.net/SSP.235.37>
- [14] J. Korzekwa et al. Tribological behaviour of Al₂O₃/inorganic fullerene-like WS₂ composite layer sliding against plastic, *Int. J. Surf. Sci. Eng.* 10 (2016) 570-584. <https://doi.org/10.1504/IJSURFSE.2016.081035>
- [15] J. Pietraszek, A. Szczotok, N. Radek. The fixed-effects analysis of the relation between SDAS and carbides for the airfoil blade traces. *Arch. Metall. Mater.* 62 (2017) 235-239. <https://doi.org/10.1515/amm-2017-0035>
- [16] J. Pietraszek. Fuzzy regression compared to classical experimental design in the case of flywheel assembly, *LNAI 7267 LNAI* (2012) 310-317. https://doi.org/10.1007/978-3-642-29347-4_36

- [17] J. Pietraszek. The modified sequential-binary approach for fuzzy operations on correlated assessments, LNAI 7894 (2013) 353-364. https://doi.org/10.1007/978-3-642-38658-9_32
- [18] J. Pietraszek et al. Non-parametric assessment of the uncertainty in the analysis of the airfoil blade traces, METAL 2017 – 26th Int. Conf. Metall. Mater. (2017) 1412-1418. ISBN 978-8087294796
- [19] J. Pietraszek, L. Wojnar. The bootstrap approach to the statistical significance of parameters in RSM model, ECCOMAS Congress 2016 Proc. 7th Europ. Congr. Comput. Methods in Appl. Sci. Eng. 1 (2016) 2003-2009. <https://doi.org/10.7712/100016.1937.9138>
- [20] J. Pietraszek et al. Challenges for the DOE methodology related to the introduction of Industry 4.0. Prod. Eng. Arch. 26 (2020) 190-194. <https://doi.org/10.30657/pea.2020.26.33>
- [21] P. Jonšta et al. The effect of rare earth metals alloying on the internal quality of industrially produced heavy steel forgings, Materials 14 (2021) art.5160. <https://doi.org/10.3390/ma14185160>
- [22] N. Radek et al. The impact of laser welding parameters on the mechanical properties of the weld, AIP Conf. Proc. 2017 (2018) art.20025. <https://doi.org/10.1063/1.5056288>
- [23] N. Radek et al. Technology and application of anti-graffiti coating systems for rolling stock, METAL 2019 – 28th Int. Conf. Metall. Mater. (2019) 1127-1132. ISBN 978-8087294925
- [24] N. Radek et al. Microstructure and tribological properties of DLC coatings, Mater. Res. Proc. 17 (2020) 171-176. <https://doi.org/10.21741/9781644901038-26>
- [25] N. Radek et al. Influence of laser texturing on tribological properties of DLC coatings, Prod. Eng. Arch. 27 (2021) 119-123. <https://doi.org/10.30657/pea.2021.27.15>